Annals of Nuclear Medicine (2020) 34:629–635
https://doi.org/10.1007/s12149-020-01486-3

ORIGINAL ARTICLE

Feasibility study of a PET-only amyloid quantification method: a comparison with visual interpretation

Natsumi Shimokawa[1] · Go Akamatsu[2] · Miyako Kadosaki[3,4] · Masayuki Sasaki[1]

Received: 16 March 2020 / Accepted: 8 June 2020 / Published online: 13 June 2020

Abstract

Objective Visual evaluation is the standard for amyloid positron emission tomography (PET) examination, though the result depends upon the physician's subjective review of the images. Therefore, it is expected that objective quantitative evaluation is useful for image interpretation. In this study, we examined the usefulness of the quantitative evaluation of amyloid PET using a PET-only quantification method in comparison with visual evaluation.

Methods In this study we retrospectively investigated a total of 166 individuals, including 58 cognitively normal controls, 62 individuals with mild cognitive impairment, and 46 individuals with early Alzheimer's disease. They underwent ^{11}C-Pittsburgh compound-B (PiB) PET examination through the Japanese Alzheimer's Disease Neuroimaging Initiative (J-ADNI). Amyloid accumulation in cerebral cortices was assessed using visual and quantitative methods. The quantitative evaluation was performed using the adaptive template method and empirically PiB-prone region of interest, and the standardized uptake value ratio (SUVR) in each area was obtained.

Results Visual evaluation and SUVR were significantly correlated in the cerebral cortices ($\rho = 0.85$–0.87; $p < 0.05$). In visual evaluation, sensitivity, specificity, and accuracy were 78%, 76%, and 77%, respectively. Meanwhile, for quantitative evaluation, sensitivity, specificity, and accuracy were 77%, 79%, and 78% in mean cortical SUVR (mcSUVR) and 79%, 79%, and 79% in maximum SUVR (maxSUVR), respectively.

Conclusion The PET-only quantification method provided a concordant result with visual evaluation and was considered useful for amyloid PET.

Keywords Amyloid PET · Alzheimer's disease · Visual evaluation · Quantitative evaluation

Introduction

In Japan, the number of people with dementia was about 4.62 million in 2012 [1, 2] and is expected to increase to about seven million by 2025. It is estimated that dementia will develop in one-fifth of elderly people aged 65 years or older. Alzheimer's disease (AD) is the most common form of dementia, and its prevalence is estimated to reach about five million people in 2025 [1, 3]. This growth in the number of patients with AD is expected to lead to huge medical costs and social burdens. Although there are no available fundamental therapeutic agents for AD, cholinesterase inhibitors that inhibit the decomposition of acetylcholine temporarily are shown to improve cognitive function and suppress the progression of symptoms [4]. Thus, early diagnosis and early intervention are expected to decrease the social burden.

In the pathological process of AD, various abnormalities occur with the disease progression. Accumulation of amyloid-β (Aβ) plaque, which forms senile plaque, is believed to begin more than 10 years before the clinical symptoms manifest [5]. Amyloid PET imaging can estimate the density of senile plaques in the brain noninvasively [6–9]. ^{11}C-Pittsburgh compound-B (^{11}C-PiB) is a widely used amyloid PET radiopharmaceutical developed

Data used in preparation of this article were obtained from the Japanese Alzheimer's Disease Neuroimaging Initiative (J-ADNI) database deposited in the National Bioscience Database Center Human Database, Japan (Research ID: hum0043.v1, 2016). As such, the investigators within J-ADNI contributed to the design and implementation of J-ADNI and/or provided data but did not participate in analysis or writing of this report. A complete listing of J-ADNI investigators can be found at: https://humandbs.biosciencedbc.jp/en/hum0043-j-adni-authors.

✉ Masayuki Sasaki
msasaki@hs.med.kyushu-u.ac.jp

Extended author information available on the last page of the article

at the University of Pittsburgh [10]. A standard for clinical practice in amyloid PET is the qualitative interpretation of accumulation, whether it is visually positive or negative [6–12]. However, visual evaluation is subjective and causes both inter- and intra-interpretation variability [13]. Although the usefulness of quantitative evaluation in clinical practice has not been established, clinical research and clinical trials have employed quantitative evaluation using standardized uptake value ratio (SUVR) [6–11].

Amyloid PET quantification typically requires spatial normalization. Although MRI is often used for spatial normalization, high-resolution three-dimensional MRI is not always available in clinical practice. Additionally, MRI-based quantification sometimes results in errors in the process of gray matter segmentation and co-registration between MRI and PET images. Therefore, an adaptive template method for amyloid PET spatial normalization was developed. This method utilizes amyloid positive and negative PET templates and does not require the MRI [12]. Some previous studies adopted either manually defined regions of interest (ROIs), automatic-anatomical-labeling ROIs or FreeSurfer-based ROIs [14–17]. However, since they are not restricted to the regions where amyloid PET drugs accumulate specifically, these anatomical ROIs would not be suitable for amyloid quantification. To solve this issue, we also developed empirically PiB-prone ROI (EPP-ROI), which is specialized for Aβ deposition in PiB PET images. A pilot study to examine the PET-only amyloid quantification with adaptive templates and EPP-ROI suggested its potential usefulness as an adjunct to visual interpretation [12]. However, this previous study preliminarily evaluated a small number of ^{11}C-PiB PET and measured only a mean cortical SUVR (mcSUVR). In the visual interpretation of ^{11}C-PiB PET, each of the four cortical regions is individually classified as positive, equivocal, and negative [13]. Not only mcSUVR but also regional SUVRs should be investigated in order to clarify the feasibility of the PET-only amyloid quantification method as a support tool for visual interpretation.

The purpose of this study was to examine the usefulness of the PET-only amyloid quantification method and to compare outcomes of visual and quantitative evaluations of amyloid PET using subjects in the Japanese Alzheimer's Disease Neuroimaging Initiative (J-ADNI) multicenter study.

Methods

Subjects

Data used in preparation of this article were obtained from the J-ADNI database deposited in the National Bioscience Database Center Human Database, Japan (Research ID: hum0043.v1, 2016) [18]. The J-ADNI was launched in 2007 as a public–private partnership, led by Principal Investigator Takeshi Iwatsubo, MD. The primary goal of J-ADNI has been to test whether serial MRI, PET, other biological markers, and clinical and neuropsychological assessment can be combined to measure the progression of late mild cognitive impairment (MCI) and mild AD in the Japanese population. The J-ADNI study is a multi-institutional joint research project on the subject of AD in Japan. A total of 537 subjects are registered, and imaging examinations and laboratory tests were performed. Amyloid PET examinations were conducted in 203 cases. The J-ADNI study was approved by the ethics committee of participating centers, and all subjects had signed an informed consent form for the retrospective data analysis of this kind. Separately, in this study, we examined 166 subjects who underwent ^{11}C-PiB PET in the J-ADNI study. Subjects consisted of 58 normal controls (NC), 62 patients with MCI, and 46 patients with AD (Table 1). This study is retrospective and was approved by the ethics committee of Kyushu University (No. 29-83).

Data acquisition and image reconstruction

The subjects received intravenous injection of 555 ± 185 MBq of ^{11}C-PiB and PET dynamic scan for

Table 1 Characteristics of subjects

Clinical diagnosis	NC	MCI	AD
The number of subjects (M/F)	58 (30/28)	62 (30/32)	46 (21/25)
Age (years)	66.4 ± 4.51 (60–80)	71.4 ± 5.45 (60–82)	74.4 ± 6.31 (62–84)
Diagnosis criteria			
NINCDS-ADRDA	–	–	Probable AD
MMSE-J	24–30	24–30	20–26
CDR-J	0	0.5	0.5 or 1.0
WMS-R	–	Below cutoff	–

NC normal control, *MCI* mild cognitive impairment, *AD* Alzheimer's disease, *NINCDS-ADRDA* National Institute of Neurological and Communicative Disorders and the Alzheimer's Disease and Related Disorders Association, *MMSE-J* Mini Mental State Examination-J, *CDR-J* Clinical Dementia Rating Scale-J, *WMS-R* Wechsler Memory Scale-Revised Logical Memory II

70 min followed immediately after injection. Data were acquired using nine PET scanners and seven PET/CT scanners. The PET images were reconstructed using 20-min data at 50 min post-injection. The attenuation correction for stand-alone PET cameras was performed by transmission scan using the segmentation method for six minutes, while that of hybrid PET/CT cameras was performed by CT scan. As regards image reconstruction conditions for amyloid PET in the J-ADNI study, the phantom examination was performed in advance, and the reconstruction condition was optimized for brain PET imaging. All the PET images acquired in each PET site went through the J-ADNI PET quality control process [18].

Image interpretation

Visual interpretation was performed by three board-certified nuclear medicine physicians well-trained in amyloid PET image interpretation. The regional uptake for four cortical areas on each side, including the frontal lobe, lateral temporal lobe, lateral parietal lobe, and precuneus/posterior cingulate, was classified as positive (2 points), equivocal (1 point), and negative (0 points). The visual interpretation criteria are described in the article by Yamane et al. [13].

Quantitative evaluation of ^{11}C-PiB PET

Quantitative evaluation was performed using SUVR, which was the uptake ratio of each region to the reference region. The reference region was the cerebellar cortex. The mcSUVR was the mean SUVR in the entire ROI, while the maxSUVR was the maximum value of four regional SUVRs in the following regions: precuneus/posterior cingulate, frontal lobe, temporal lobe lateral side and parietal lobe lateral side. Both quantitative evaluation and visual interpretation were used to examine the same four regions.

Figure 1 shows the workflow of the PET-only amyloid quantification method [12]. The PET images were spatially normalized using the adaptive template method. The images were normalized to both the positive and negative templates, respectively. The transformation vector for a template that most resembles the image was adopted. The EPP-ROI that developed based on the ^{11}C-PiB accumulated area in patients with AD was inversely transformed using a transformation vector and placed on the individual PET in native space. Image processing was performed with PMOD version 3.7 (PMOD Technologies, Zürich, Switzerland).

Statistical analyses

JMP Pro 13 (SAS Institute Inc., Cary, USA) was used for statistical analyses. Correlation between visual and quantitative evaluation was analyzed using Spearman's rank correlation coefficient with a p value of < 0.05 as statistically significant. Receiver operating characteristics curve (ROC) analysis was used to calculate the SUVR cutoff value for differentiating normal and diseased subjects.

Results

The results of the visual evaluation in relation to clinical diagnosis are shown in Fig. 2. Among the NC subjects, 44 (75.9%) were amyloid PET negative and 14 (24.1%) showed either positive or equivocal. Among the MCI subjects, 21 (33.9%) were negative and 41 (66.1%) were either positive or equivocal. Finally, in patients with AD, 3 (6.5%) were negative and 43 (93.5%) were either positive or equivocal. When MCI and AD were considered to be a disease, the

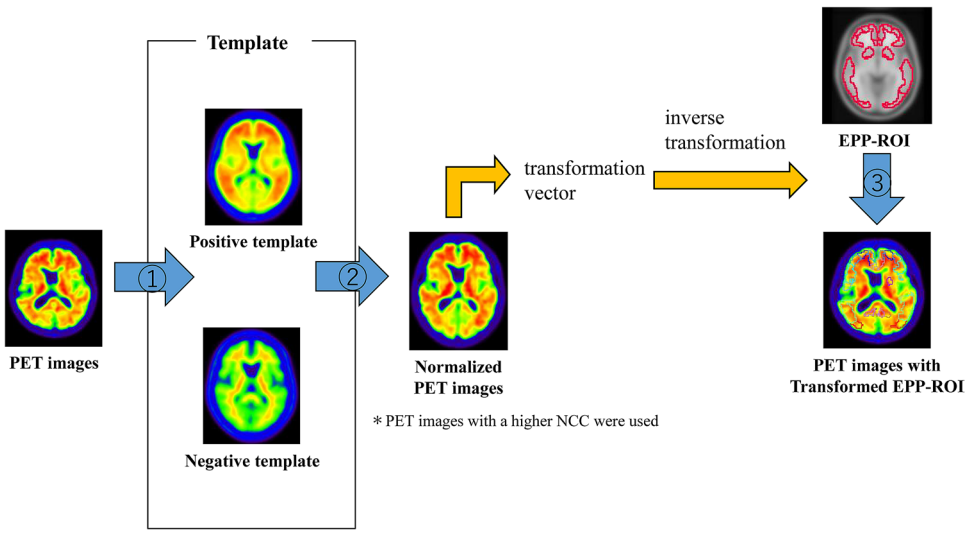

Fig. 1 Scheme of the PET-only amyloid quantification method. Transformation vectors for templates that more closely resemble the images were adopted. EPP-ROI was inversely transformed using a transformation vector and placed on the individual PET scans (*NCC* normalized cross-correlation, *EPP-ROI* empirically PiB-prone region of interest)

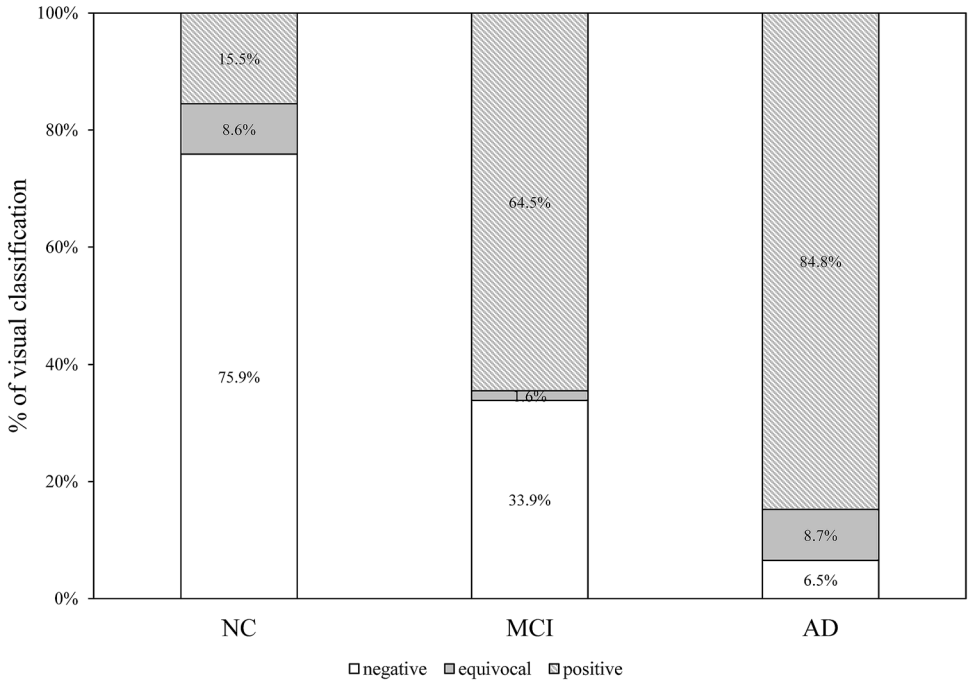

Fig. 2 Visual evaluation of subjects in relation to clinical diagnosis. Most of the subjects with NC were PET-negative, while most with MCI and AD were PET-positive

Table 2 Comparison of the diagnostic accuracy for differentiation

	Sensitivity	Specificity	Accuracy
Visual evaluation	78% (84/108)	76% (44/58)	77% (128/166)
mcSUVR	77% (83/108)	79% (46/58)	78% (129/166)
maxSUVR	79% (85/108)	79% (46/58)	79% (131/166)

mcSUVR mean cortical standardized uptake value ratio, *maxSUVR* maximum SUVR

sensitivity, specificity, and accuracy were, respectively, 78%, 76%, and 77% (Table 2).

Figure 3 shows the relationship between regional visual interpretation and regional SUVR in each region. When the visual point of regional uptake was high, the SUVR was also high. Spearman's rank correlation coefficient was significant ($\rho = 0.86$; $p < 0.05$). Significant correlations were also observed in the precuneus/posterior cingulate ($\rho = 0.87$; $p < 0.05$), the frontal lobe ($\rho = 0.87$; $p < 0.05$), the lateral temporal lobe ($\rho = 0.86$; $p < 0.05$), and the lateral parietal lobe ($\rho = 0.85$; $p < 0.05$).

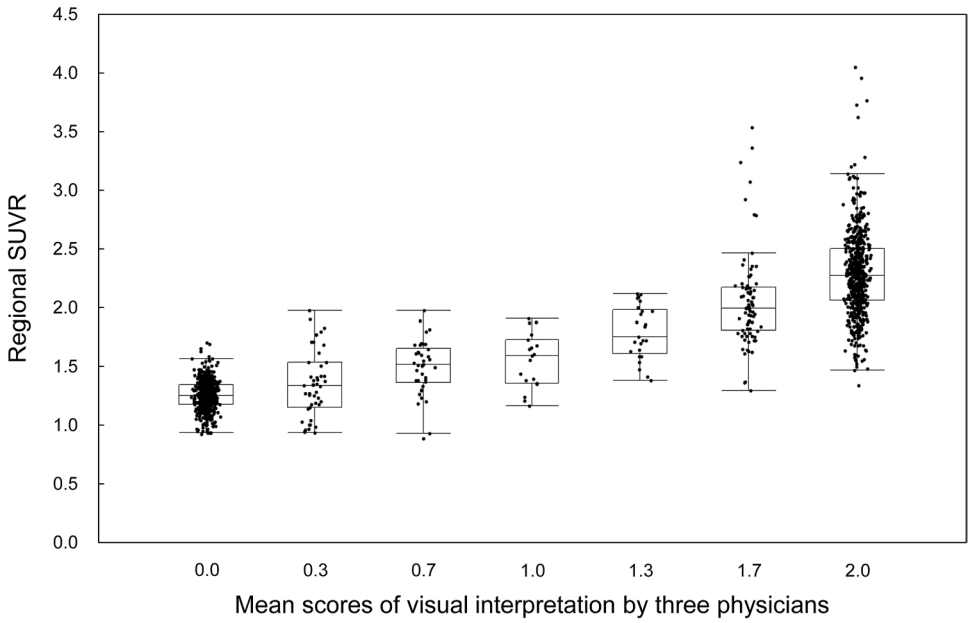

Fig. 3 Relationship between visual interpretation and regional SUVR. Spearman's rank correlation coefficient for each region was $\rho = 0.87$ for the precuneus/posterior cingulate ($p < 0.05$), $\rho = 0.87$ for the frontal lobe ($p < 0.05$), $\rho = 0.86$ for the lateral temporal lobe ($p < 0.05$), and $\rho = 0.85$ for the lateral parietal lobe ($p < 0.05$)

Figure 4 shows the relationship between visual and quantitative evaluation by patient group. The cutoff value for differentiating between visually negative and both positive and equivocal results were calculated by ROC analysis. Cutoff values were 1.41 for mcSUVR and 1.59 for maxSUVR. Concordant results between visual and quantitative evaluation were obtained as 157 of 166 cases (94.6%) for mcSUVR and 158 of 166 cases (95.2%) for maxSUVR. In 98 subjects with visually positive or equivocal, 7 subjects were negative using mcSUVR and 6 subjects were negative using maxSUVR. Among the 68 subjects with visually negative results, 1 subject was positive using mcSUVR and no subjects were positive using maxSUVR. The mcSUVR values of negative, equivocal, and positive outcomes were 1.25 ± 0.11, 1.39 ± 0.20, and 2.17 ± 0.34, respectively. The difference in mcSUVR among visual classifications was significant ($p < 0.05$). Separately, the maxSUVR values of negative, equivocal, and positive results were 1.35 ± 0.13, 1.56 ± 0.21, and 2.48 ± 0.41, respectively ($p < 0.05$).

The comparison of diagnostic accuracy between visual and quantitative evaluation is shown in Table 2. The sensitivity, specificity, and accuracy when using visual evaluation were 78%, 76%, and 77%, respectively. Additionally, they were 77%, 79%, and 78% using mcSUVR and were 79%, 79%, and 79% using maxSUVR, respectively. In comparison with visual evaluation, one true-positive subject decreased and two true-negative subjects increased using mcSUVR, while one true-positive subject increased and two true-negative subjects increased using maxSUVR. Finally, the diagnostic accuracy of quantitative evaluation was almost equal to that of visual evaluation. The clinical diagnosis by maxSUVR tended to be a little higher than that when using visual evaluation and mcSUVR, though the difference was not statistically significant.

Discussion

In this study, we examined the usefulness of a PET-only amyloid quantification method and compared the results with the visual evaluations. This method was consisted of an adaptive template spatial normalization method and an EPP-ROI. In the area specialized for Aβ deposition, visual evaluation and SUVR were highly correlated. Compared with visual evaluation, the diagnostic accuracy for differentiation in the quantitative evaluation was almost equivalent.

In the precuneus/posterior cingulate, frontal lobe, temporal lobe lateral side, and parietal lobe lateral side, visual interpretation and SUVR were highly correlated ($\rho = 0.85$–0.87). Further, the concordance rates between quantitative evaluation and visual evaluation were 94.6% in mcSUVR and 95.2% in maxSUVR. Thurfjell et al. reported that the concordance rate between quantitative value (SUVR) and the visual evaluation of ^{18}F-flutemetamol PET images was 97.1–99.4% [19], which was consistent with our results.

The sensitivity, specificity, and accuracy were about 75–80% in both visual evaluation and quantitative evaluation. Using amyloid PET, Jack et al. [20] reported that 30% of NC, 60% of MCI, and 85–90% of AD subjects were positive. The diagnostic accuracy of our study was almost the same as that reported by Jack et al. In quantitative evaluation by maxSUVR, the sensitivity, specificity, and accuracy tended to be slightly higher than those of visual evaluation. A subject with MCI who was visually negative became positive when assessed by maxSUVR. Conversely, two subjects with NC who were visually equivocal became negative when assessed by maxSUVR. Elsewhere, Yamane et al. [13] also compared visual and quantitative evaluations using the J-ADNI data and reported that some amyloid-negative cases with low mcSUVR were interpreted as positive by visual evaluation. The authors concluded that quantitative evaluation was useful, especially for subjects with mild amyloid

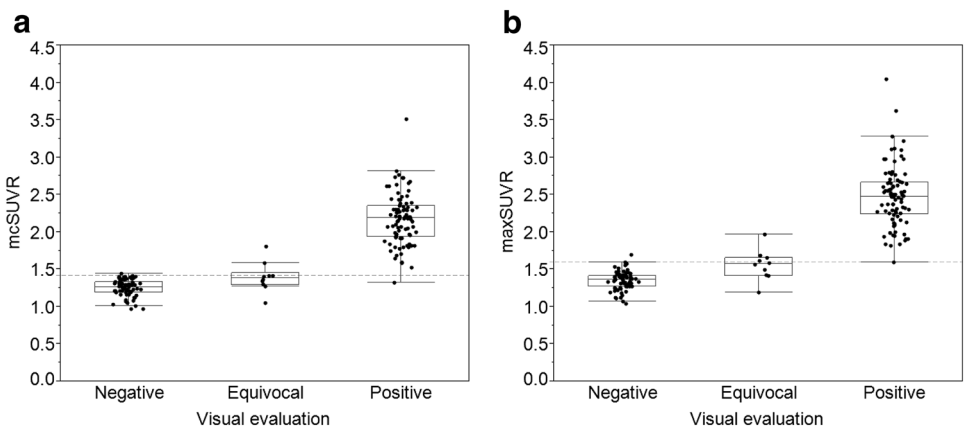

Fig. 4 Relationship between visual evaluation and SUVR (**a** mcSUVR, **b** maxSUVR). Dashed lines indicated cutoff values. The difference among visual classification was significant ($p < 0.05$)

accumulation with an SUVR of around 1.5. In our study, when the SUVR was around the threshold, quantitative evaluation showed slightly higher diagnostic accuracy than that of visual evaluation. These results suggest that quantitative evaluation using amyloid PET is useful to a similar degree as with visual evaluation for diagnosing AD and may even show an advantage in the differentiation of subjects with borderline accumulation. Furthermore, Vandenberghe et al. [21] reported that test–retest variabilities of regional SUVRs were 1–4%, so quantitative evaluation can be expected to yield high reproducibility. More examinations with more subjects are required.

In this study, the diagnostic accuracy of maxSUVR was concordant with both the visual evaluation and mcSUVR. Compared to mcSUVR, one more subject was found to be true positive using maxSUVR. The mcSUVR was the average of SUVR in whole regions, while the maxSUVR was the highest SUVR among the four regions. In cases with PiB accumulation in a small limited area, using mcSUVR, which is an average of a wider area, was considered to cause the underestimation. Because the visual classification results were positive with PiB accumulation in only two gyri, maxSUVR is considered to provide similar results to visual classification. Thurfjell et al. [19] reported that the concordance with visual classification was slightly higher in SUVR calculated by small and narrow composite regions as compared with larger ones. Large regions are considered to be more affected by partial-volume effects. The maxSUVR may improve sensitivity for the evaluation of amyloid PET.

There were some limitations in the present study. First, the diagnostic accuracy was not significantly different between the modalities; therefore, it is necessary to increase the number of cases. Second, the examination of subjects with more advanced AD may provide different results. Lastly, ^{18}F-labeled pharmaceuticals received regulatory approval recently. We should examine the usefulness of our method for ^{18}F-labeled amyloid PET in the future.

Conclusion

PET-only amyloid quantification method is comparably useful to visual evaluation for diagnosing AD. The concordance rates between visual interpretation and quantitative evaluation were 94.6% in mcSUVR and 95.2% in maxSUVR. The quantification of amyloid PET would be useful, especially for subjects with mild Aβ plaque accumulation in the brain.

Acknowledgements J-ADNI was supported by the following grants: Translational Research Promotion Project from the New Energy and Industrial Technology Development Organization of Japan; Research on Dementia, Health Labor Sciences Research Grant; Life Science Database Integration Project of Japan Science and Technology Agency; Research Association of Biotechnology (contributed by Astellas Pharma Inc., Bristol-Myers Squibb, Daiichi-Sankyo, Eisai, Eli Lilly and Company, Merck-Banyu, Mitsubishi Tanabe Pharma, Pfizer Inc., Shionogi & Co., Ltd., Sumitomo Dainippon, and Takeda Pharmaceutical Company), Japan, and a grant from an anonymous foundation.

Funding None.

Compliance with ethical standards

Conflict of interest The authors declare that they have no competing interests.

References

1. Ninomiya T. Japan Prospective Studies Collaboration for Aging and Dementia (JPSC-AD). Brain Nerve. 2017;69:763–9.
2. Health and Labour Sciences Research Grant. Dementia research project. 2013. https://www.tsukuba-psychiatry.com/wp-content/uploads/2013/06/H24Report_Part1.pdf. (in Japanese) Accessed 27 May 2020.
3. Akatsu H, Takahashi M, Matsukawa N, Ishikawa Y, Kondo N, Sato T, et al. Subtype analysis of neuropathologically diagnosed patients in a Japanese geriatric hospital. J Neurol Sci. 2002;196:63–9.
4. McGleenon BM, Dynan KB, Passmore AP. Acetylcholinesterase inhibitors in Alzheimer's disease. Br J Clin Pharmacol. 1999;48:471–80.
5. Bateman R, Xiong C, Benzinger T, Fagan AM, Goate A, Fox NC, et al. Clinical and biomarker changes in dominantly inherited Alzheimer's disease. N Engl J Med. 2012;367:795–804.
6. Clark CM, Pontecorvo MJ, Beach TG, Bedell BJ, Coleman RE, Doraiswamy PM, et al. Cerebral PET with florbetapir compared with neuropathology at autopsy for detection of neuritic amyloid-beta plaques: a prospective cohort study. Lancet Neurol. 2012;11:669–78.
7. Clark CM, Schneider JA, Bedell BJ, Beach TG, Bilker WB, Mintun MA, et al. Use of florbetapir-PET for imaging beta-amyloid pathology. JAMA. 2011;305:275–83.
8. Curtis C, Gamez JE, Singh U, Sadowsky CH, Villena T, Sabbagh MN, et al. Phase 3 trial of flutemetamol labeled with radioactive fluorine 18 imaging and neuritic plaque density. JAMA Neurol. 2015;72:287–94.
9. Sabri O, Sabbagh MN, Seibyl J, Barthel H, Akatsu H, Ouchi Y, et al. Florbetaben PET imaging to detect amyloid plaques in Alzheimer disease: Phase 3 study. Alzheimers Dement. 2015;11:964–74.
10. Lopresti BJ, Klunk WE, Mathis CA, Hoge JA, Ziolko SK, Lu X, et al. Simplified quantification of Pittsburgh Compound B amyloid imaging PET studies: a comparative analysis. J Nucl Med. 2005;46:1959–72.
11. Rinne JO, Brooks DJ, Rossor MN, Fox NC, Bullock R, Klunk WE, et al. 11C-PiB PET assessment of change in fibrillar amyloid-beta load in patients with Alzheimer's disease treated with bapineuzumab: a phase 2, double-blind, placebo-controlled, ascending-dose study. Lancet Neurol. 2010;9:363–72.
12. Akamatsu G, Ikari Y, Ohnishi A, Nishida H, Aita K, Sasaki M, et al. Automated PET-only quantification of amyloid deposition with adaptive template and empirically pre-defined ROI. Phys Med Biol. 2016;61:5768–80.
13. Yamane T, Ishii K, Sakata M, Ikari Y, Nishio T, Ishii K, et al. Inter-rater variability of visual interpretation and comparison with quantitative evaluation of 11C-PiB PET amyloid images of the

Japanese Alzheimer's Disease Neuroimaging Initiative (J-ADNI) multicenter study. Eur J Nucl Med Mol Imaging. 2017;44:850–7.
14. Zhou L, Salvado O, Dore V, Bourgeat P, Raniga P, Macaulay SL, et al. MR-less surface-based amyloid assessment based on 11C PiB PET. PLoS ONE. 2014;9:e84777.
15. Bourgeat P, Villemagne VL, Dore V, Brown B, Macaulay SL, Martins R, et al. Comparison of MR-less PiB SUVR quantification methods. Neurobiol Aging. 2015;36(Suppl 1):S159–S166166.
16. Su Y, D'Angelo GM, Vlassenko AG, Zhou G, Snyder AZ, Marcus DS, et al. Quantitative analysis of PiB-PET with FreeSurfer ROIs. PLoS ONE. 2013;8:e73377.
17. Saint-Aubert L, Nemmi F, Péran P, Barbeau EJ, Payoux P, Chollet F, et al. Comparison between PET template-based method and MRI-based method for cortical quantification of florbetapir (AV-45) uptake in vivo. Eur J Nucl Med Mol Imaging. 2014;41:836–43.
18. Iwatsubo T, Iwata A, Suzuki K, Ihara R, Arai H, Ishii K, et al. Japanese and North American Alzheimer's Disease Neuroimaging Initiative studies: harmonization for international trials. Alzheimers Dement. 2018;14:1077–87.
19. Thurfjell L, Lilja J, Lundqvist R, Buckley C, Smith A, Vandenberghe R, et al. Automated quantification of 18F-flutemetamol PET activity for categorizing scans as negative or positive for brain amyloid: concordance with visual image reads. J Nucl Med. 2014;55:1623–8.
20. Jack CR Jr, Lowe VJ, Senjem ML, Weigand SD, Kemp BJ, Shiung MM, et al. 11C-PiB and structural MRI provide complementary information in imaging of Alzheimer's disease and amnestic mild cognitive impairment. Brain. 2008;131:665–80.
21. Vandenberghe R, Laere KV, Ivanoiu A, Salmon E, Bastin C, Triau E, et al. 18F-flutemetamol amyloid imaging in Alzheimer disease and mild cognitive impairment: a phase 2 trial. Ann Neurol. 2010;68:319–29.

Affiliations

Natsumi Shimokawa[1] · Go Akamatsu[2] · Miyako Kadosaki[3,4] · Masayuki Sasaki[1]

[1] Division of Medical Quantum Science, Department of Health Sciences, Graduate School of Medical Sciences, Kyushu University, 3-1-1 Maidashi, Higashi-ku, Fukuoka 812-8582, Japan

[2] National Institute of Radiological Sciences (NIRS), National Institutes for Quantum and Radiological Science and Technology (QST), 4-9-1 Anagawa, Inage-ku, Chiba 263-8555, Japan

[3] Department of Health Sciences, Faculty of Medical Sciences, Kyushu University, 3-1-1 Maidashi, Higashi-ku, Fukuoka 812-8582, Japan

[4] Department of Radiological Technology, Kyushu Central Hospital, 3-23-1 Shiobaru, Minami-ku, Fukuoka 812-8588, Japan